Spin-wave dispersion and sublattice magnetization in NiCl$_2$

Spin-wave dispersion and sublattice magnetization in NiCl$_2$

P A Lindgård†‡, R J Birgeneau†‡, J Als-Nielsen‡ and H J Guggenheim†

† Bell Laboratories, Murray Hill, New Jersey, USA
‡ Danish AEC Research Establishment, Risø, Roskilde, Denmark

Abstract. NiCl$_2$ is a Heisenberg planar antiferromagnet composed of hexagonal ferromagnetic Ni^{2+} sheets with effective XY symmetry weakly coupled antiferromagnetically to adjacent Ni^{2+} sheets. The near two-dimensionality implies a directionally-dependent spin-wave renormalization together with an unusual temperature dependence of the sublattice magnetization, gap energy and specific heat. In this paper we report an inelastic neutron scattering study of the spin waves both at low temperatures and, for selected q-vectors, for temperatures up to $T_N = 52.3$ K. The sublattice magnetization has been measured from 1.5 K to T_N. A renormalized spin-wave theory, which does not contain any assumptions about the temperature dependence of the energy gap, has been developed. Previous experiments have given a between-plane exchange $J' = -0.77$ K and a planar anisotropy constant $D = 0.40$ K. From the in-plane dispersion relation we deduce $J_{NN} = 21.70$ K and $J_{NNN} = -4.85$ K ($\mathcal{H} = -2\Sigma_{i>j} J_{ij} S_i . S_j$). Using these interaction constants and the renormalized spin-wave theory, the temperature-dependent dispersion relations (together with the sublattice magnetization) and the gap energy up to ~ 0.4 T_N are properly predicted.

1. Introduction

The transition metal dihalides FeCl$_2$, CoCl$_2$ and NiCl$_2$ have been of considerable interest for many decades (Cabrera 1918, Landau 1933, Bizette *et al* 1956 and Néel 1957). These compounds originally attracted attention because they represent archetypes of that special class of materials known as 'metamagnets' which exhibit an antiferromagnetic state which can be ferromagnetically saturated in relatively weak magnetic fields. This behaviour, first explained by Landau (1933), originates in the fact that these crystals, all of which have the CdCl$_2$ structure, are composed of strongly-coupled ferromagnetic sheets of spins with successive planes weakly coupled antiferromagnetically. Thus a modest applied field can overcome the weak between-plane coupling to induce a transition from an antiferromagnetic to a ferromagnetic state. More recently, because of current interest in both the phase transition problem and lower dimensional systems (for a review see de Jongh and Midiema, 1974), it has been the near two-dimensionality of these materials which has attracted interest.

The differences in the magnetic properties of these three compounds arise mainly from differences in the anisotropies. In FeCl$_2$ and CoCl$_2$ the orbital moment is only partially quenched so that both systems have large anisotropy—of Ising symmetry in the former (Birgeneau *et al* 1972) and XY symmetry in the latter (Hutchings 1973). In NiCl$_2$, on the other hand, the anisotropy is extremely small, $H_A/H_E \sim 3 \times 10^{-3}$, and of XY symmetry. Thus NiCl$_2$ corresponds closely to a model system with a nearly isotropic spin Hamiltonian but with large spatial anisotropy in the interaction strengths. As emphasized

by Silberglitt (1973) in his work on $CrBr_3$, such systems supply sensitive and critical tests to the theory of spin-wave interaction effects. In particular, because of the two-dimensional character, the spin-wave dispersion surface is very anisotropic with a low-lying branch for wavevectors in the direction of weak forces. Thus even at temperatuers much less than T_N, spin waves in that direction will be strongly populated and consequently will interact significantly. Ideally, the between-plane forces should be weak enough so that the dispersion surface is highly anisotropic but, on the other hand, of sufficient strength that the dispersion in the soft direction can be measured with conventional neutron scattering techniques. $NiCl_2$ provides a rather good example of such a system. As an aside we should also mention $NiCl_2$ has been extensively investigated via microwave resonance techniques, especially with respect to the critical behaviour (Lozenko *et al* 1971, Birgeneau *et al* 1973, Birgeneau and Rupp 1974). In this case $NiCl_2$ is of special interest because it is a non-cubic system with a nearly isotropic spin Hamiltonian; the near two-dimensionality is then of secondary interest.

In this paper we report a detailed neutron scattering study of the spin-wave dispersion relations in $NiCl_2$. Measurements of the sublattice magnetization as a function of temperature from 1·5 K to $T_N = 52·3$ K are also reported. A selfconsistent renormalized spin wave theory, which does not contain any assumptions about the temperature dependence of the gap, is developed. All available data are analysed using this model and the interaction constants thus deduced. It is found that simple spin-wave theory gives a good description of all low-temperature properties and, with renormalization effects included, of the sublattice magnetization and the gap up to about 0·4 T_N. The format of the paper is as follows. Section 2 gives preliminary details such as the crystal and magnetic structure and estimation of exchange constants based on pre-existing data. The renormalized spin-wave theory is presented in §3. The experimental results and analyses are given in §4 and finally the discussion and conclusions are given in §5.

2. Preliminary details

The crystal and magnetic structure of $NiCl_2$ are illustrated in figure 1. The primitive nuclear cell is rhombohedral, space group D_{3d}^5 with one molecule per unit cell. This crystal structure may in fact be generated from the rock salt structure by removing alternate sheets of metal atoms along the [111] axis. The near two-dimensionality of the magnetism is immediately evident from the crystal structure itself. In this study it is more convenient to use a double hexagonal cell with 6 formula units per unit volume. In this double cell the Ni^{2+} ions sit at $(0, 0, 0)$, $(0, 0, \frac{1}{2})$, $(\frac{1}{3}, \frac{2}{3}, \frac{1}{3})$, $(\frac{1}{3}, \frac{2}{3}, \frac{5}{6})$, $(\frac{2}{3}, \frac{1}{3}, \frac{1}{6})$ and $(\frac{2}{3}, \frac{1}{3}, \frac{2}{3})$ and the Cl ions are at each of these $\pm(0, 0, \frac{1}{2}u)$ where $u \simeq 0.25$. The lattice constants for our samples at 4·2 K are $a = 3·468 \pm 0·01$ Å and $c_{2h} = 34·40 \pm 0·04$ Å.

From various antiferromagnetic resonance experiments in $NiCl_2$ it has been inferred that the magnetic structure is characterized by ferromagnetic sheets of spins with successive planes antiferromagnetically aligned. It is also believed that the spins lie in the hexagonal plane as indicated in figure 1. We have not carried out a comprehensive structure study. However, our neutron diffraction data are consistent with this proposed structure; because of the multidomain of our samples it was not possible to determine the spin direction in the hexagonal plane.

For the spin-wave calculation we shall treat $NiCl_2$ as a simple antiferromagnet with two atoms per unit cell. The Hamiltonian may then be written in the form
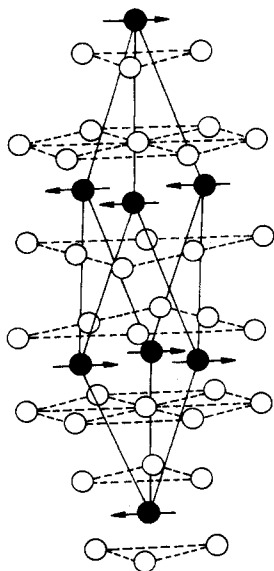
Figure 1. Crystal and magnetic structure of NiCl$_2$. Open circle, chlorine ion; full circle, nickel ion.

$$\mathscr{H} = - \sum_{i>j} 2J_{ij}S_i \cdot S_j - \sum_{i>j'} 2J'_{ij'}S_i \cdot S_{j'} - D \sum_i S_i^{x^2} - D' \sum_i (S_i^{y^2} - S_i^{z^2}).$$ (1)

Here the crystalline a axis is chosen as the axis of quantization and J_{ij} and J'_{ij} refer to intra- and interplanar interactions respectively. If $D = D' > 0$ the anisotropy favours the plane perpendicular to the z direction; for $D > D'$ the x direction is preferred. We shall discuss the possible microscopic contributions to D, D' in §3 and §5. From the antiferromagnetic resonance studies it is known that at 4·2 K NiCl$_2$ exhibits a low frequency in-plane mode at essentially 0 cm^{-1} (Birgeneau and Rupp 1974) and a high frequency out-of-plane mode at 3·73 K (Lozenko *et al* 1971, Katsumata and Yamasaka 1973). It is known in addition that the transition from the antiferromagnetic to a saturated ferromagnetic state at 4·2 K occurs for a field $H^z = 129$ kG (de Gunzbourg *et al* 1971). As discussed by Katsumata and Yamasaka (1973), this gives

$$D = D' = 0·40 \text{ K}$$

and

$$J' = -0·77 \text{ K}$$ (2)

where we have assumed nearest neighbours between-plane interactions alone. This value for J' may be compared with Lines' (1963) value of $J' = -0·73$ K deduced from $\chi_\perp$. Thus D, D' and J' appear to be rather well known. The in-plane interactions are rather more difficult to estimate. From the neutron scattering results in FeCl$_2$ and CoCl$_2$ it is expected that both nearest (J_{NN}) and next nearest (J_{NNN}) neighbours interactions will be important. From a Green's function calculation of T_N Lines (1963) estimates $J_{NN} \sim 9·5$ K, while from the temperature dependence of the gap Katsumata and Yamasaka (1973) estimate $J_{NN} \sim 11·5$ K. An alternative approach is to approximate NiCl$_2$ as an ideal two-dimensional system and to estimate the exchange via the Stanley–Kaplan (1966) formula for T_c: this yields $J_{NN} + J_{NNN} = 17·4$ K. As we shall see, this latter estimate is much closer to the correct value. The ratio of the intraplanar to interplanar interaction then is about 23 : -1 so that NiCl$_2$ should indeed exhibit highly anisotropic spin-wave dispersion relations; on the other hand the critical behaviour should be fully three-dimensional.

Before discussing the experimental results we consider first the renormalized spin-wave theory for a system described by equation (1).

3. Renormalized spin wave theory

The spin-wave theory for a system described by equation (1) may be developed using conventional techniques (see for example Narath and Davis 1965, Marshall and Lovesey 1971, Rastelli *et al* 1974, Lindgård and Danielsen 1975). Using the Holstein–Primakoff transformation of spin operations to Bose operators we obtain a Hamiltonian having $0, 2, 4, \ldots$ Bose operators. We shall restrict ourselves to this. Diagonalizing the quadratic term of $\mathcal{H}$ yields the following unrenormalized spin-wave energies:

$$E_m^2(q) = A_q^2 - (B + (-1)^m D_q)^2$$

where $m = 1$ gives the acoustic branch and $m = 2$ gives the optic branch. $A_q = 2S(J_0 - J_q + J_0' + D(1 - 1/2S))$, $B = -2SD'(1 - 1/2S)$ and $D_q = 2S|J_q'|$. In the following we shall use the notation $J_q = \Sigma_p J_p \gamma_q^p$ with $\gamma_q^p = \Sigma \exp(i\boldsymbol{q}.\boldsymbol{\delta}_p)$, $\boldsymbol{\delta}_p$ being the vector in the plane to the pth neighbour group. We use a similar definition of $J_q' = J'\gamma_q'$.

The spin-wave renormalization is calculated in the Hartree–Fock approximation by decoupling the four Bose operator terms directly (Lindgård and Danielsen 1975). We then find new temperature-dependent coefficients to the quadratic Hamiltonian given as:

$$A_q(T) \pm B(T) + (-1)^m D_q(T) = 2S\{\sum_p J_p(\gamma_0^p - \gamma_q^p)(1 - R_1^p(T)) + J'(\gamma_0' + (-1)^m \gamma_q')$$

$$\times (1 - R_2(T)) + (D \mp D')(1 - 1/2S)(1 - 2R_3(T) \pm R_4(T))\}$$

which gives the energies $E_m^2(q, T) = A_q^2(T) - (B(T) + (-1)^m D_q(T))^2$.

The temperature dependence is described by the wavevector-independent functions $R_i(T)$, in which the temperature dependence enters via the population factors $\langle n_q^m \rangle = \{\exp(E_m(q, T)/kT) - 1\}^{-1}$. They are defined as follows:

$$R_1^p(T) = \frac{1}{2SN} \sum_{q,m} \left(1 - \frac{\gamma_q^p}{\gamma_0^p}\right) a_q^m \langle n_q^m \rangle$$

$$R_2(T) = \frac{1}{2SN} \sum_{q,m} \left(a_q^m + (-1)^m \frac{\gamma_q'}{\gamma_0'} x_q^m\right) \langle n_q^m \rangle$$

$$R_3(T) = \frac{1}{2SN} \sum_{q,m} a_q^m \langle n_q^m \rangle$$

$$R_4(T) = \frac{1}{2SN} \sum_{q,m} x_q^m \langle n_q^m \rangle$$

where $a_q^m = A_q(T)/E_m(q, T)$, $x_q^m = -(B(T) + (-1)^m D_q(T))/E_m(q, T)$ and N is the number of atoms per sublattice. We have neglected operator terms (ab) in the decoupled interaction Hamiltonian which are not present in the quadratic Hamiltonian and furthermore terms involving the averages corresponding to R_1^p with a_q^m replaced by x_q^m. Both types of terms only contribute to second order in the renormalization. For $NiCl_2$ they contribute less than 1 % to the renormalization.

The above theory is not restricted to two-dimensional systems. In special cases such as the pure ferro- or antiferromagnet, $E_m(q, T)$ reduces to that calculated by many authors,

that is, the spin waves in both cases renormalize proportional to the spin-wave energy. In the general case with finite anisotropy and both ferro- and antiferromagnet interaction, the renormalization depends on the wavevector in a more complicated fashion. The temperature variation of the sublattice magnetization is given by $M = g\mu_B(S' - R_3(T)S)$, where S' is the spin corrected for the zero point deviation ($S' = 0.999$ for NiCl$_2$).

The two-dimensional character of NiCl$_2$ has a number of consequences which may be traced in the expressions for the spin-wave energies and the renormalization. Spin waves propagating along the c axis have low energies because the interplane interaction is small. Thermal population of these spin-wave states takes place at low temperatures and the spin-wave energies renormalize strongly. The in-plane spin waves have high energies; they are weakly populated and, as they do not couple directly with the c axis spin waves, their renormalization is very small. The sublattice magnetization depends on the total population of spin-wave states and there is a substantial reduction already at low temperatures due to population of the c axis spin waves.

The present theory contains no assumptions about ideal two-dimensionality, as in the case of Katsumata and Yamasaka (1973). This is important for a quantative comparison with experiment. The isostructural compound FeCl$_2$, which was recently discussed theoretically by Lovesey (1974) and Rastelli *et al* (1974), differs essentially since in this system the temperature dependence of the energy gap, which is produced by a large single-ion anisotropy term, completely describes the spin-wave renormalization. The two-dimensional character plays a smaller rôle for the spin-wave renormalization in FeCl$_2$ in contrast to NiCl$_2$.

The main rôle of the single-ion anisotropy is to produce an energy gap at $q = 0$ in the dispersion relation of the upper mode. Since the renormalization factors $R_i(T)$ via both the population factor and the state vector factors a_q^m and x_q^m are especially sensitive to the low-energy parts of the dispersion surface it is essential to include the renormalization of the energy gap selfconsistently. This was not the case in the theory by Narath and Davis (1965) in which the energy gap was assumed to vary as the sublattice magnetization.

For the case of planar anisotropy ($D = D'$) one spin-wave branch must go to zero at zero wavevector according to the Goldstone theorem. For NiCl$_2$ a direct numerical calculation of the dipolar sums shows that the dipole interaction completely accounts for the planar anisotropy. We shall discuss the significance of this in §5. The contribution from one sublattice to A_q and B_q for hexagonal symmetry with q along the hexagonal axes and the spin along the x axis, in the plane, is

$$A_{qz}^{dip} = - S(g\mu_B)^2 \sum_r \frac{1}{r^3}\left(1 - \frac{3x^2}{r^2}\right)(1 + \frac{1}{2}\cos(q_z z))$$

$$B_{qz}^{dip} = S(g\mu_B)^2 \sum_r \frac{1}{r^3}\left(1 - \frac{3x^2}{r^2}\right)\frac{3}{2}\cos(q_z z)$$

where $r = (x, y, z)$ is a vector to another spin in the same sublattice. The direct calculation shows that the contribution from the other sublattice is an order of magnitude smaller and that the variation with q of A_{qz} and B_{qz} is less than 15 %. Since only contributions for $q = (0, 0, q_z)$ are important (otherwise the isotropic exchange is dominant) we see that the single-ion planar anisotropy model is excellent for describing the effect of the dipolar interaction. Furthermore the dipolar forces favour the spin direction to be in the hexagonal plane.

The numerical calculation of the spin-wave renormalization, the sublattice magnetization and the specific heat for NiCl$_2$ was performed as follows. The q-summation in-

volved in the temperature-dependent factors $R_i(T)$ was taken over the irreducible part of the Brillouin zone using a coarse mesh (9000 points/BZ) away from $q = (0, 0, q)$ and a fine mesh (45 000 points/BZ) in $\frac{1}{4}$ of the zone around this line, where the energies are low. The numerically singular point $q = (0, 0, 0)$ was excluded from the sum since it has no weight for $N \to \infty$. Selfconsistency was obtained after 2–3 iterations.

4. Experimental results

The experiments were carried out mainly on a disc-shaped sample $3 \times 13 \times 20$ mm which had in turn been cleaved from a much larger single-crystal boule. The $NiCl_2$ used for the crystal growth was prepared by reacting 99·999 % Ni sponge with anhydrous hydrogen chloride up to 900°C. The chloride was recrystallized by sublimation and then sealed in a quartz crystal-growing crucible. The crystal was grown in a standard Bridgeman furnace by lowering the crucible through a temperature gradient at 1·0 mm per hour. It should be noted that the quartz crucible was preheated in a HCl atmosphere at 1000°C before filling. This treatment prevents the wetting of the quartz by the chloride which, when cooled, causes cracking of the crystal and crucible. Some preliminary measurements were also carried out on a crystal grown by J Makovsky and kindly lent to us by E Cohen.

The experiments were performed on a triple-axis spectrometer at the Riso DR 3 Reactor using conventional constant-Q techniques. A four-inch high curved graphite crystal was used as a monochromator and the analyser was a flat graphite crystal.
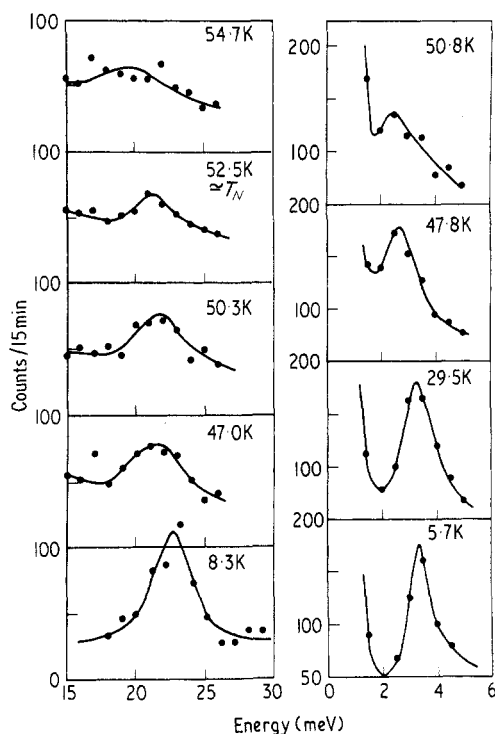

Figure 2. Typical spin-wave scans in $NiCl_2$ at the in-plane zone boundary, $Q_x = 1·05\,\text{Å}^{-1}$ (left-hand part) and 1/3 of the way to the zone boundary, $Q = 0·35\,\text{Å}^{-1}$ (right-hand part).

Typical experimental results for the in-plane magnons as a function of temperature are shown in figure 2. These were taken with constant energy out, $E_f = 13.7$ meV, using a pyrolytic graphite filter to remove higher order neutrons; the measurements were performed away from the (101) magnetic reciprocal lattice position (see insert in figure 3). The low temperature $(q, 0, 0)$ dispersion relation thus determined is shown in figure 3. The curves are the result of unrenormalized spin-wave theory with

$$J_{NN} = 21.7\ K, \qquad J_{NNN} = -4.85\ K. \tag{3}$$

It is evident that the dispersion relation is accurately accounted for including only NN and NNN interactions. From (3) we have $J_{NN} + J_{NNN} = 16.9$ K; this is quite close to our Stanley–Kaplan value of 17.4 K deduced by approximating NiCl$_2$ as an idealized two-dimensional system.
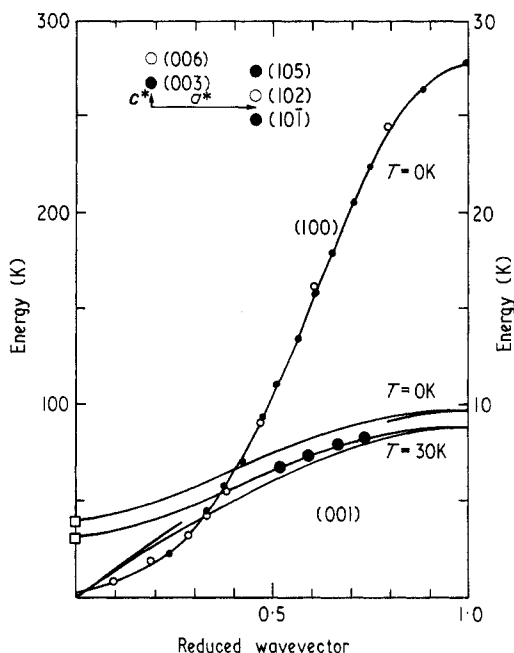

Figure 3. Spin-wave dispersion for NiCl$_2$ in the (100) direction (left-hand scale) and the (001) direction (right-hand scale) in a double-zone scheme. The curves are from theory and the points $\circ$ from neutron scattering data and $\square$ from NMR data. $J_{NN} = 21.70$ K, $J_{NNN} = -4.85$ K, $J' = -0.77$ K and $D = 0.40$ K. Inserted is a section of the reciprocal space.

Measurements of spin waves propagating along the c axis proved to be rather more difficult. These measurements were taken at $E_i = 5$ meV, scanning E_f in order to obtain the necessary resolution. The neutron flux is then diminished drastically and in order to gain intensity from the population factor in the cross section these measurements were carried out at 30 K. Bragg scattering contamination prevented data at $\xi > 0.75$. The 30 K dispersion relation is shown in figure 3. The theoretical curves represent a renormalized spin-wave calculation using the independently determined parameters found from (1) and (3). It is evident that the agreement is excellent.

The theoretical renormalization of the [100] zone boundary spin wave is 2.7% at $T = 40$ K. This should be compared with the renormalization of the [001] zone boundary
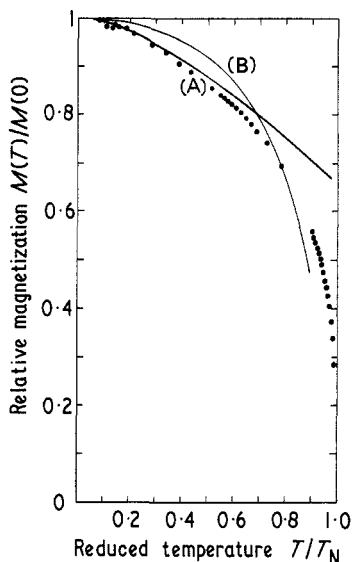
Figure 4. Sublattice magnetization of $NiCl_2$. The results of the renormalized theory, curve (A), and molecular field theory, curve (B), are shown (S = 1).
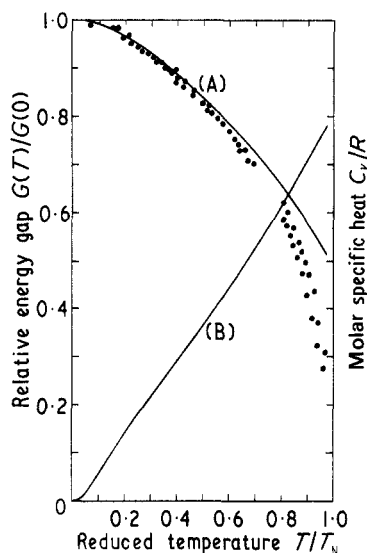
Figure 6. Spin-wave energy gap, left scale. The curve (A) is from theory and the experimental points (•) are taken from Katsumata and Yamasaka (1973); a better agreement is obtained here than is obtained by their approximate two-dimensional theory. The calculated molar specific heat is also shown, curve (B), right scale. Notice the weak Shottky anomaly at $T/T_N \sim 0.2$, ie $T \sim 10$ K.
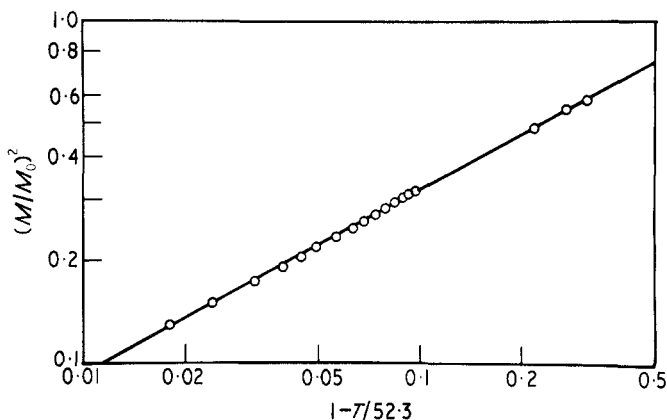

Figure 5. Critical behaviour of the reduced sublattice magnetization squared in $NiCl_2$. The full line is the result of a least squares fit to the data with $2\beta = 0.54$.

spin wave, which is theoretically 22% at the same temperature. The experimental renormalization of the [100] zone boundary spin wave is shown in figure 2. It is 2–3 % at $T = 40$ K—in good agreement with the theory.

The sublattice magnetization in arbitrary units was obtained by the magnetic (009) Bragg scattering for $T \geqslant 5$ K. A detailed study at 1·2 K and 4·2 K (using (105) and (10$\bar{1}$)) gave an upper bound of 1 % in the increase in the magnetization over this temperature

interval. Systematic errors and possible extinction are estimated to be less than 2%. The magnetization data scaled to best fit with the theory is shown in figure 4. Before discussing the spin-wave calculations we consider briefly the critical behaviour. From $dI(009)/dT$ we estimate $T_N \sim 52 \cdot 3$ K; a least-squares fit of the intensity data between 36 K and 51·4 K to a power law yields the results shown in figure 5. The critical exponent $\beta = 0 \cdot 27$ is close to that found in FeCl$_2$, $\beta = 0 \cdot 29$, by Birgeneau *et al* (1972) and is clearly characteristically three-dimensional.

5. Discussion

The renormalized spin-wave theory in the Hartree–Fock (HF) approximation is compared with experimental data in figures 3, 4 and 6. It is evident from figure 3 that the dispersion curves are very anisotropic with respect to the direction of q resulting in an unusual density of states, figure 7, with a high density at small energies. This gives rise to the rapid
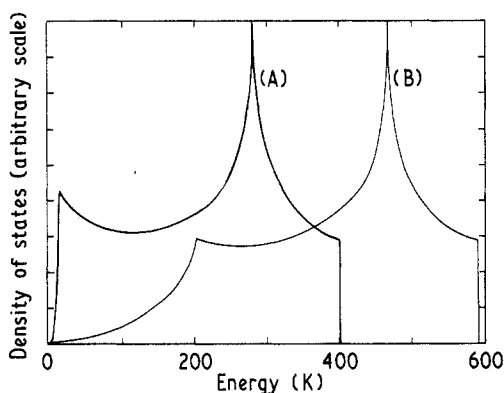

Figure 7. The spin-wave density of states for NiCl$_2$, curve (A), and for an isotropic magnet with $-J' = J_{NN} + J_{NNN}$; curve (B), $J_{NN} = 21 \cdot 70$ K, $J_{NNN} = -4 \cdot 85$ K, $J' = -0 \cdot 77$ K and $D = 0 \cdot 40$ K.

decrease in the magnetization, figure 4, and the energy gap, figure 6. With no adjustable parameters we obtain an excellent agreement up to 40% of T_N, at which point the HF approximation and the Holstein–Primakoff transformation to second order become insufficient. It is clear that very significant deviations set in around 10% below T_N due to the critical fluctuations. This is in agreement with the preliminary results and analysis (Lingård *et al* 1974) in which a different theoretical approach was used. The interaction Hamiltonian was first transformed to noninteracting spin-wave operators and then decoupled in the HF approximation. The difference between that and the present approach is of second order in the renormalization.

    The renormalization is dominated by the $R_3(T)$ function, which gives the reduction of the relative magnetization (figure 4). The ratios are—for all but very low temperatures—approximately

$$R_1^1 : R_1^2 : R_2 : R_3 : R_4 = 2:4:8:12:1.$$

This means that the renormalized spin-wave energies for NiCl$_2$ are very well given by the zero-temperature formula with temperature-dependent parameters scaled according to power laws of the sublattice magnetization.

The magnetic contribution to the molar specific heat was calculated and is shown on the right-hand scale of figure 6. It shows a small 'Shottky anomaly' near 10 K on a parabolic background. The resulting temperature dependence is close to linear over a large region, a behaviour which was recently observed experimentally(Kostryuwa 1974). The Shottky anomaly is associated with the interplane excitations and the concomitant peak in the density of states near 10 K. For illustrative purposes the density of states is also shown for the hypothetical magnet with equal antiferro- and ferromagnetic interaction $(-J' = J_{NN} + J_{NNN}$, curve (B) in figure 7). We notice that the density associated with the in-plane excitations is almost rigidly shifted whereas the interplane density is smeared out. Such a magnet has clearly a much less renormalization relative to T_N.

Finally, we consider the $NiCl_2$ interaction parameters themselves. The basic pattern of the exchange constants is identical in each of $FeCl_2$, $CoCl_2$ and $NiCl_2$. In all three cases J_{NN}, which proceeds via a 90° Cl^- superexchange link, is strong and ferromagnetic while J_{NNN}, which proceeds via a double Cl^- bridge, is weaker and antiferromagnetic in both $FeCl_2$ and $NiCl_2$. In all three cases the between-plane exchange, which again takes place via two intervening Cl^- ligands, is weak and antiferromagnetic. The ratios of intra- to interplanar exchange $(J_{NN} + J_{NNN})/J'$, in $FeCl_2$, $CoCl_2$ and $NiCl_2$ are -20, -13 and -23 respectively. It is evident that the sign and relative values of the exchange constants are not especially sensitive to the particular 3d configuration involved. The rather weak anisotropy in $NiCl_2$ is somewhat more puzzling. As we have noted previously the anisotropy parameter $D = 0·40$ K coincides precisely with that expected from the magnetic dipole interaction above. On the other hand, it is known from EPR that for Ni^{2+} in the isostructural compound $CdCl_2$, D (single ion) $= 1·0$ K (Orton, 1959). One might also have expected a comparable contribution in the concentrated material from anisotropic exchange since the Ni^{2+} orbital moment is not fully quenched $(g = 2·24)$. We must conclude therefore that in $NiCl_2$ these latter two contributions fortuitously cancel at $q = 0$ thus producing the small anisotropy observed.

Acknowledgment

References

Birgeneau R J, Rupp L W Jr, Guggenheim H J, Lindgård P A and Huber D L 1973 *Phys. Rev. Lett.* **30** 1252
Birgeneau R J and Rupp L W Jr 1974 *Proc. Int. Conf. on Magnetism, Moscow 1973* (Moscow: Izdatelstvo 'Nauka') 4 287
Birgeneau R J, Yelon W B, Cohen E and Makovsky J 1972 *Phys. Rev.* **B5** 2607
Bizette H, Terrier C and Tsai B 1956 *C.R. Acad. Sci., Paris* **243** 1295
Cabrera B 1918 *J. Chim. Phys.* **16** 442
de Gunzbourg J, Papassimacopoulos S, Mieden-Gros A and Allain A 1971 *J. Phys., Paris* **32** CI 125
de Jongh L J and Miedema A R 1974 *Adv. Phys.* **23** 1
Hutchings M T 1973 *J. Phys. C: Solid St. Phys.* **6** 3143
Katsumata K and Yamasaka K 1973 *J. Phys. Soc. Japan* **34** 346
Kostryuwa M O 1974 *Proc. Int. Conf. on Magnetism, Moscow 1973* (Moscow: Izdatelstvo 'Nauka')
Landau L 1933 *Z. Phys. Sowjun.* **4** 675
Lindgård P A, Als-Nielsen J, Birgeneau R J and Guggenheim H J 1974 *Proc Int. Conf. on Magnetism, Moscow 1973* (Moscow: Izdatelstvo 'Nauka')

Lindgård P A and Danielsen O 1975 *Phys. Rev.* B **11** 351 and *J. Phys.* C: *Solid St. Phys.* **7** 1523
Lines M E 1963 *Phys. Rev.* **131** 546
Lovesey S W 1974 *J. Phys.* C: *Solid St. Phys.* **7** 2049
Lozenko A F, Malinoskii V I and Ryabchenko S M 1971 *Zh. Eksp. Teor. Fiz.* **60** 1387
Marshall W and Lovesey S W 1971 *Theory of thermal neutron scattering* (London: Oxford UP) p 253
Narath A and Davis H L 1965 *Phys. Rev.* A **137** 163
Orton J W 1959 *Rep. Prog. Phys.* **22** 204
Rastelli E, Tassi A and Reatto L 1974 *J. Phys.* C: *Solid St. Phys.* **7** 1735
Silberglitt R 1973 *A.I.P. Conf. Proc.* **18** 754
Stanley H E and Kaplan T A 1966 *Phys. Rev. Lett.* **17** 913